2011 American Control Conference
on O'Farrell Street, San Francisco, CA, USA
June 29 - July 01, 2011

Model-based detection of a moving gaseous source in a 2D spatial domain using a sensor-based grid adaptation approach

Michael A. Demetriou Nikolaos A. Gatsonis Jeffrey R. Court

Abstract— **The release of gases from land or aerial-based vehicles into an environment represents accidental or deliberate action. This work considers the dispersion of a plume from a moving source and proposes a model-based estimation scheme that provides the proximity of the source location by means of a guided mobile agent that carries a sensor. The method couples grid refinement with estimation and includes a kinematic model for the mobile agent. Using Lyapunov-based method, a stable guidance scheme is provided for the spatial relocation of the moving sensor. Computational results serve to demonstrate the effectiveness of the method for 2D spatial domains and realistic parameters for the source, mobile agent, and ambient conditions.**

Index Terms— **Plume dispersion; moving source; mobile sensors; PDEs; grid adaptation**

I. Introduction

The dispersion of a plume from a stationary or moving source into the atmosphere is representative of accidental or deliberate release of gases from land- or aerial-based vehicles. The detection of the source using a mobile sensor is a problem that has been under consideration with a variety of approaches [1], [2], [3], [4], [5], [6].

The dispersion of the released gas under certain physical conditions can be modeled by an advection-diffusion PDE with spatially and time varying ambient mean velocity and eddy diffusivities. In this work, we present a model-based detection scheme that has an advantage over other approaches because it provides an estimate of the source location *and* simultaneously reconstructs the state, i.e. the concentration field. Our approach combines the sensor relocation with process state estimation and grid adaptation in order to address gas dispersion processes with spatiotemporally varying parameters. This approach advances significantly previous work [6], [7], [8] and provides a new abstract framework that couples estimation and computational schemes.

The theoretical model includes a sensor affixed on a mobile sensing agent (MSA) which is used to obtain measurements of the process state. The diffusion state and source location estimation are obtained with a finite volume implementation on structured, non-uniform, adaptive grids. The model of the process uses the measurement information to estimate the process state and the proximity of the moving source, and subsequently dictate the spatial relocation of the moving sensor. The grid is adapted based on estimates of the source location in order to improve accuracy and speed-up the estimation process. This new grid adaptation approach results in a switched dynamical system for the state estimator.

In this paper we present the theoretical model, the algorithms, the numerical implementation, and numerical results obtained with a set of gas release conditions in 2D. The computational parameters used in the simulations are representative of realistic conditions for the atmosphere, the source, and the MSA.

The authors are with Worcester Polytechnic Institute, Dept of Mechanical Engineering, Worcester, MA 01609, USA, {mdemetri,gatsonis,jeff.court}@wpi.edu. The authors gratefully acknowledge financial support from the AFOSR, grant FA9550-09-1-0469.

II. Physical model

The diffusion process of a gaseous substance released in an incompressible atmosphere with mean wind velocity $W(t,\mathbf{r}) = (W_X, W_Y)$ is described by the advection-diffusion transport equation for the mean concentration $c(t,\mathbf{r})$ of the trace species over a spatial domain $\Omega \subset \mathbb{R}^2$

$$\frac{\partial c}{\partial t} + u\frac{\partial c}{\partial X} + v\frac{\partial c}{\partial Y} + w\frac{\partial c}{\partial Z} = \frac{\partial}{\partial X}\left(K_{XX}\frac{\partial c}{\partial X}\right) + \frac{\partial}{\partial Y}\left(K_{YY}\frac{\partial c}{\partial Y}\right) + \frac{\partial}{\partial Z}\left(K_{ZZ}\frac{\partial c}{\partial Z}\right) + S(t,\mathbf{r}), \tag{1}$$

where the eddy diffusivities are $K_{XX}(t,\mathbf{r}), K_{YY}(t,\mathbf{r})$, $K_{ZZ}(t,\mathbf{r})$, $S(t,\mathbf{r})$ is the source term, and $\mathbf{r} = (X,Y) \in \mathbb{R}^2$ is the Cartesian coordinate vector. Associated with the above equation are the appropriate boundary conditions which for this case assume zero concentration at the boundaries, $c|_{\partial\Omega} = 0$. We assume that the gas release occurs from a moving aerial vehicle and the equation models a plume that has time to reach the diffusive stage. We are also concerned with time scales that are smaller than the diurnal variations of the atmospheric parameters and there are no chemical interactions, [9], [10], [11].

For a 2D realization considered in this paper with the spatial domain given by the rectangle $\Omega = [0, L_X] \times [0, L_Y] \subset \mathbb{R}^2$, the source term is given by $S(t,X,Y) = b(X,Y)f(t)$ where $f(t)$ denotes the release rate and $b(X,Y)$ denotes the spatial location of the source; the latter in terms of system theoretic description is also referred to as the spatial distribution of the source term. It is often assumed that the manner in which the source enters the spatial domain is that of a pointwise source; this then can be mathematically represented by spatial Dirac delta function

$$b(X,Y) = \delta(X - X_c)\delta(Y - Y_c) \tag{2}$$

where (X_c, Y_c) is the centroid of the source location. A moving source can then be described by a *time varying*

centroid $(X_c(t), Y_c(t))$. Using the above, one may rewrite the above PDE as follows

$$\frac{\partial c}{\partial t} + u\frac{\partial c}{\partial X} + v\frac{\partial c}{\partial Y} = K_{XX}\frac{\partial^2 c}{\partial X^2} + K_{YY}\frac{\partial^2 c}{\partial Y^2} + bf. \quad (3)$$

A. Sensor model

Information on the concentration is realized via a sensor attached to a mobile agent which provides (noise-corrupted) values of the concentration $c(t, X, Y)$ at a spatial point (X_s, Y_s) of the domain Ω. Therefore an adequate sensor model takes the form

$$y(t) = c(t, X_s, Y_s) = \int_0^{L_X}\int_0^{L_Y} \delta(X - X_s)\delta(Y - Y_s)c(t, X, Y)\, dX\, dY. \quad (4)$$

To incorporate the effects of a possibly moving sensing device, the sensor centroid is explicitly taken to be time-dependent and thus

$$y(t) = \int_0^{L_X}\int_0^{L_Y} \delta(X - X_s(t))\delta(Y - Y_s(t))c(t, X, Y)\, dX\, dY.$$

B. Mobile sensing agent kinematics and control

The guidance scheme proposed in the subsequent section represents the velocities that the mobile sensing agent *ought* to have. Certainly when one assumes a mass-less and inertia-less sensor-plus-vehicle, then the above guidance velocities are assumed. However, when the assumption of a point sensor is removed, one may use the following 2D kinematics of a fixed-wing aircraft that is equipped with a standard low level autopilot as in [12]. The vehicle's position and orientation can be described with the Cartesian coordinates (X, Y) and the heading angle $\psi(t)$,

$$\begin{cases} \dot{X}(t) = v(t)\cos(\psi(t)) \\ \dot{Y}(t) = v(t)\sin(\psi(t)) \\ \dot{\psi}(t) = \omega_\psi(t) \end{cases} \quad (5)$$

where $\omega_\psi(t)$ is the commanded turning rate of the aerial vehicle and $v(t)$ is the commanded velocity. While the above kinematic equations are identical to those for terrain robots [13], the MSA will have to satisfy additional constraints on the commanded signals and which are given by

$$v_{min} \le v \le v_{max}, \quad -\omega_{\psi,max} \le \omega_\psi \le \omega_{\psi,max}.$$

At the current stage, it is assumed that the sensing aerial vehicle has knowledge of its own state $(X(t), Y(t), \psi(t))$. From the desired velocities $(\dot{X}^d, \dot{Y}^d)$ produced by the estimation scheme, the desired speed and heading can be calculated as

$$v^d(t) = \sqrt{\dot{X}^d(t)^2 + \dot{Y}^d(t)^2}, \quad \psi^d(t) = \tan^{-1}\left(\frac{\dot{Y}^d(t)}{\dot{X}^d(t)}\right)$$

respectively. After enforcing the velocity limitations, the first input to the kinematic equations (5) is known. The commanded turning rate is calculated based on the desired heading and the current heading of the MSA as

$$\omega_\psi(t) = \frac{\psi^d(t) - \psi(t)}{\Delta t}$$

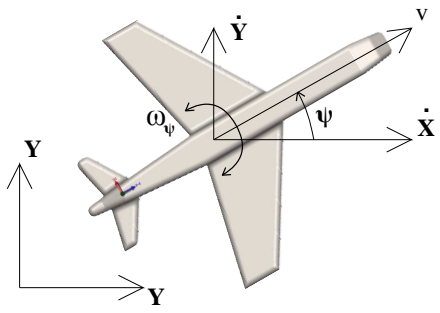

Fig. 1. Sketch of the MSA coordinate system in 2D.

where Δt is the time between command signals being sent to the MSA. After enforcing the limitations on the MSA's turning rate, the second input to the kinematic equations (5) is known.

III. Abstract formulation

The advection-diffusion PDE (3) may be written as an evolution equation in a Hilbert space. The state space in this case is taken to be $\mathcal{X} = L^2(\Omega)$. Associated with the state space, is the Sobolev space $\mathcal{V} = H^1(\Omega)$ with $\mathcal{V}$ dense in $\mathcal{X}$. The state is an element of the Hilbert space $x(t) = c(t, \cdot, \cdot)$ from $[0, T]$ in $\mathcal{V}$ and is the solution to the initial value problem

$$\begin{aligned} &\dot{x}(t) = \mathcal{A}x(t) + \mathcal{B}(\theta_c(t))f(t), \;\; x(0) = x_0 \in \mathcal{X}, \\ &y(t; \theta_s(t)) = \mathcal{C}(\theta_s(t))x(t), \end{aligned} \quad (6)$$

where $\mathcal{A}$ is the spatial operator associated with the advection diffusion operator, $\mathcal{B}$ contains the spatial information of the source, and $\mathcal{C}$ contains the spatial information of the sensor. For well-posedness, it is required that $\mathcal{B}(\theta_c(\cdot))f(\cdot) \in L^2(0, T; \mathcal{V}^*)$, see [14], [15], [16], where $\mathcal{V}^* = H^{-1}(\Omega)$ denotes the dual of $\mathcal{V}$, [17].

IV. State estimator with a moving sensing agent

Due to the specific structure of the spatial distribution of both the source term and of the moving sensor, the proposed estimator follows directly from the one proposed in [7] and is given by

$$\begin{aligned} \dot{\widehat{x}}(t) &= (\mathcal{A} - \gamma\mathcal{C}^*(\theta_s(t))\mathcal{C}(\theta_s(t)))\,\widehat{x}(t) \\ &\quad + \gamma\mathcal{C}^*(\theta_s(t))y(t; \theta_s(t)) + \mathcal{B}(\theta_s(t))f(t), \\ \widehat{x}(0) &= 0, \end{aligned} \quad (7)$$

where γ is a user defined gain used to tune the estimator and the term $\mathcal{B}(\theta_s(t))f$ represents the estimate of the source position and is defined as the location-parameterized input operator evaluated at the current sensor location $\theta_s(t)$. The above is completed with the time variation of the sensor centroid $\theta_s(t) = (X_s(t), Y_s(t))$. In order to obtain the sensor guidance, one considers the state estimation error $e(t) =$

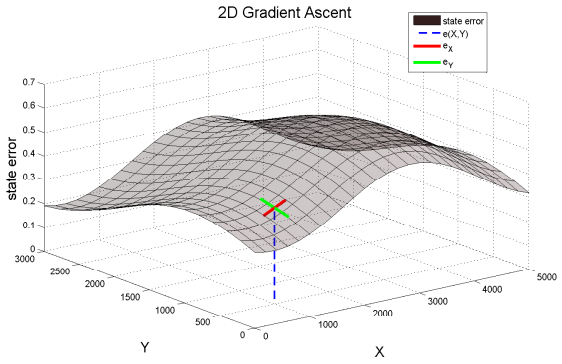

Fig. 2. Graphical interpretation of 2D gradient ascent variables.

$x(t) - \widehat{x}(t)$. It should be noted that the spatially distributed function $e(t, X, Y) = x(t, X, Y) - \widehat{x}(t, X, Y)$ when viewed as an element of the Hilbert space $\mathcal{X}$ is denoted by $e(t)$. The state error equation is given by

$$\begin{aligned} \dot{e}(t) &= \left(\mathcal{A} - \gamma \mathcal{C}^*(\theta_s(t))\mathcal{C}(\theta_s(t))\right) e(t) \\ &\quad + \left(\mathcal{B}(\theta_c(t))) - \mathcal{B}(\theta_s(t))\right) f(t), \\ e(0) &= e_0 \in \mathcal{X}. \end{aligned} \tag{8}$$

The well-posedness and stability of the above evolution system can be examined under strict conditions and will appear in a companion publication by the authors. In essence it requires that at a minimum, the forcing term in (8) above, comprised of the difference of the input operators evaluated at the true source location $\theta_c(t)$ and the sensor location $\theta_s(t)$, be square integrable.

A. Mobile sensing agent guidance

The requisite guidance policy that dictates the movement of the mobile sensing agent within the spatial domain Ω is based on Lyapunov stability analysis. We use the following notation for the spatial gradients, as they are used in the sensor guidance

$$e_X(t, X, Y) = \frac{\partial e(t, X, Y)}{\partial X}, \;\; e_Y(t, X, Y) = \frac{\partial e(t, X, Y)}{\partial Y}.$$

Using the Lyapunov-based guidance from [7], the guidance of the mobile sensing agent is given by

$$\begin{aligned} \dot{X}_s(t) &= -k_X \, e(t, X_s(t), Y_s(t)) \cdot e_X(t, X_s(t), Y_s(t)) \\ \dot{Y}_s(t) &= -k_Y \, e(t, X_s(t), Y_s(t)) \cdot e_Y(t, X_s(t), Y_s(t)) \end{aligned} \tag{9}$$

where $k_X, k_Y > 0$ are user-defined guidance gains.

Remark 1 (Gradient-based policy): The above guidance policy is essentially a *gradient policy* whose component velocities are proportional to the state error at the current sensor location $(X_s(t), Y_s(t))$ and the spatial gradients evaluated at the current sensor location $(X_s(t), Y_s(t))$. It requires the sensor to move in the direction of the greatest spatial gradients (e_X, e_Y) of the concentration error and of the greatest value of the concentration error $e(t, X, Y)$. The guidance policy requires the use of three scalar signals: the concentration error and the two spatial gradients at the sensor location $(X_s(t), Y_s(t))$ to be realized.

B. State estimate convergence

The estimation scheme outlined is a gradient based approach that drives the sensing agent in the direction of a higher state error. Due to the nature of the continuous source, a local state error will always exist in the vicinity of the source. When the source speed is slower than the maximum sensor speed, the sensor will eventually follow the source through the domain. With a source that is not continuous, a local state error will not always exist near the source. In this case, the estimation scheme will only estimate the state and will not provide an accurate estimation of the source location.

V. Numerical Implementation and Sensor-Based Grid Adaptation

A. Finite dimensional approximation of plant based on finite volume formulation

The spatial domain is discretized with a structured multigrid using rectangular cells [18]. The advection-diffusion PDE is written in strong conservative form and solved with a finite volume method (FVM). The PDE is normalized using values for density, velocity, length, time and diffusivity. The resulting PDE is then written in flux-form and integrated over a control volume. The integrations are carried out over the control-volume cells to form a system of semi-discrete equations which is integrated using the four-step Runge-Kutta scheme. The method follows the one implemented by Gatsonis et al. [19] to the compressible, viscous MHD (Navier-Stokes type) equations.

In summary, the finite dimensional approximation of the proposed estimator-plus-sensor guidance scheme given by (7), (9) is given by the finite dimensional system

$$\begin{aligned} \dot{\widehat{x}}^n(t) &= \left(A - \gamma C^T(\theta_s(t))C(\theta_s(t))\right) \widehat{x}^n(t) \\ &\quad + \gamma C^T(\theta_s(t)) y(t; \theta_s(t)) + B(\theta_s(t)) f(t) \\ \dot{X}_s(t) &= -k_X \, e^n(t, X_s(t), Y_s(t)) \cdot e^n_X(t, X_s(t), Y_s(t)) \\ \dot{Y}_s(t) &= -k_Y \, e^n(t, X_s(t), Y_s(t)) \cdot e^n_Y(t, X_s(t), Y_s(t)) \end{aligned} \tag{10}$$

where $\widehat{x}^n(t)$ denotes the finite dimensional representation of the infinite dimensional state estimate $\widehat{x}(t)$, $e^n(t, X, Y)$ denotes the finite dimensional representation of the state error and the matrices A, C, B denote the finite dimensional approximation of the operators $\mathcal{A}, \mathcal{C}, \mathcal{B}$, respectively. It should be noted that the matrix A represents the infinite dimensional operator $\mathcal{A}$ corresponding to a given grid; keeping the same dimension n but changing the grid (stretch and compress) changes the structure but not the dimension of the matrix A.

B. Finite dimensional approximation of estimator

The finite dimensional approximation of the estimator is similar to that of the plant. The domain is discretized with a structured multigrid finite volume formulation. The grids used are coarser than those used for the descretization of the

plant. The integration of the equations for the estimated state and kinematics of the MSA is also carried out with the four step Runge-Kutta scheme.

C. Sensing Aerial Vehicle deployment model

When wind direction information is available, then the MSA begins patrolling the spatial domain downwind in a circular path until the sensing device registers a value above its sensitivity threshold. If wind information is not utilized, one may consider random search in the spatial domain. Once a measurement indicating the presence of nonzero concentration is registered, then MSA changes from search-mode to estimation-mode. For the latter all guidance information then comes from the proposed estimation scheme via (9). Once the estimation scheme is activated, desired velocity information streams to the aircraft control scheme described in (5) above.

D. Sensor measurements and guidance from numerical model

The sensor assumes knowledge of state and gradient at the current spatial location. For concentration, it is assumed constant within a finite-volume cell and determined based on the current sensor location

$$c(X,Y) = c_{i,j}$$

The gradient in the X and Y directions at the position of the sensor is obtained with a second order differencing of the adjacent cell values as

$$\frac{\partial \bar{c}(X,Y)}{\partial X} = \frac{c_{i+1,j} - c_{i-1,j}}{X_{i+1,j} - X_{i-1,j}}, \quad \frac{\partial \bar{c}(X,Y)}{\partial Y} = \frac{c_{i,j+1} - c_{i,j-1}}{Y_{i+1,j} - Y_{i-1,j}}.$$

E. Sensor-based grid adaptation and switching

Modifications on the computational scheme allow for the state estimation scheme to locally stretch and compress the grid thus resulting in a switched dynamical system. This grid adjustment produces different representations of the finite dimensional approximation of the diffusion process equation thereby resulting in a two-way coupling of the computational scheme and the estimation scheme. In the system theoretic context, this resulted in a hybrid dynamical system where different constant matrices representing the original operators of the diffusion equation modeling the diffusion of concentration, are being used by the estimation scheme. The switching of the estimator matrices was dictated by the estimated position of the moving source. A pseudo code summarizing this estimation-based grid adaptation is presented in Algorithm 3 below. Figure 4 demonstrates this grid adaptation based on current sensor location.

To arrive at the hybrid system, we consider the family of matrices $\{A_i,\, i \in \mathcal{I}\}$ parameterized by the index set $\mathcal{I}$. For the specific case considered here, the set consists of nine different matrices, all of the same dimension and each representing a refined grid that is covers 25% of the spatial domain, while the remaining 75% is coarse grid, see Figure 4. We let $\sigma : [0,\infty) \to \mathcal{I}$ be a piecewise constant function of time (the switching signal). Associated with the above nine choices of the state matrices A are the output vectors $C_i(\theta)$. Now, let $(S_p)_{p\in\mathcal{I}}$ be a family of linear continuous time systems, which for each fixed $p \in \mathcal{I}$ is given by

$$\begin{aligned}\dot{\widehat{x}}^n(t) = &\left(A_p - \gamma C_p^T(\theta_s(t))C_p(\theta_s(t))\right)\widehat{x}^n(t) \\ &+\gamma C_p^T(\theta_s(t))y(t;\theta_s(t)) + B_p(\theta_s(t))f(t)\end{aligned} \tag{11}$$

To this family $(S_p)_{p\in\mathcal{I}}$ we associate the set

$$\Sigma = \left\{\sigma \,\middle|\, \sigma : [t_0,\infty) \to \mathcal{I} \text{ piecewise constant}\right\}$$

for all possible switches between the above nine systems. The *family of switched systems* $((S_p)_{p\in\mathcal{I}}, \Sigma)$ taken under consideration are the hybrid dynamical systems consisting of the family of continuous time systems $(S_p)_{p\in\mathcal{I}}$ together with all switching rules $\sigma \in \Sigma$, all initial states $\widehat{x}^n(0) = \widehat{x}_0^n$. For each given switching function σ, denote the finite set of switching time instants associated to σ by $t_0 < t_1 < t_2 < \ldots$, where $k(\sigma) \in \mathbb{N} \setminus \{0\}$. Here, $k(\sigma) - 1$ denotes the number of discontinuities for the piecewise continuous function σ, i.e. the number a refined grid is switched in.

In view of the above formulation, the switching time instants depend on current sensor position; if the sensor is in a region of finer grid, then switch to the (A_p, C_p) that correspond to that grid, Figure 4.

F. Implementation pseudo code and flowchart

The simulations for this work are run in two separate parts as shown in Figure 3. The first part is to generate a set of plant data in the absence of experimental data and save the results to a file. This is the most time consuming part of the simulation and is all completed before the estimation scheme begins. In practice and application, the first part of the simulation would be replaced by MSA measurements of the atmosphere. The second part of the simulation is the actual estimation scheme. The estimator uses small pieces of this stored data as measurement readings throughout the estimation process. The pseudo code for this entire process is outlined below.

Algorithm 1 Forward Problem

```
read simulation parameters
discretize high dimensional uniform grid
for t = dt to t_final do
    calculate (X, Y)_c
    RK4 integration of x
    apply type 1 BC
end for
output state at each time to file
```

VI. Computational results

Several simulations were run to demonstrate the performance of this approach. Initially, the source is placed in the domain at a location where it will benefit from the known wind profile. The simulation begins with the source

Algorithm 2 Estimation Scheme

Require: Output data from forward problem.

read simulation parameters
generate switched system grids
known $(X, Y, \psi)_s$
for $t = dt$ to t_{final} **do**
  read $c(X_s, Y_s, t)$, $\frac{\partial c(X_s,Y_s,t)}{\partial X}$, $\frac{\partial c(X_s,Y_s,t)}{\partial Y}$
  if $c(X, Y, \psi) \geq y_{min}$ **then**
    if request command signal **then**
      $\dot{X}(t) \leftarrow k_X e(t, X_s(t), Y_s(t)) e_X(t, X_s(t), Y_s(t))$
      $\dot{Y}(t) \leftarrow k_Y e(t, X_s(t), Y_s(t)) e_Y(t, X_s(t), Y_s(t))$
      adjust $(\dot{X}(t), \dot{Y}(t)$ for constraints
    end if
    RK4 integration of $\hat{x}$
    apply type 1 BC
  else
    continue patrol
  end if
  calculate $(X, Y)_s$ new
  switch grid
end for

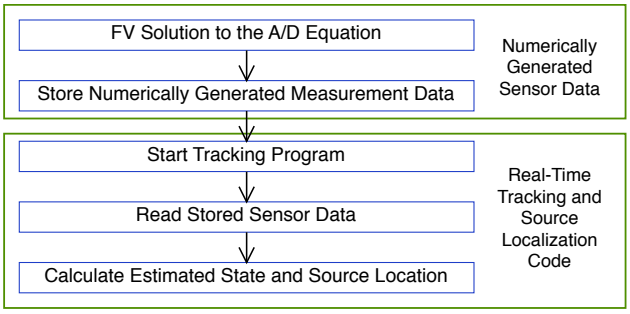

Fig. 3. Simulation Flow Chart.

patrolling a small area and taking measurements. While patroling, the system assumes no source is present. As soon as the sensor detects a disturbance in the form of a concentration above a minimum threshold, the estimation scheme starts.

For all cases, the sensor speed is constrained to $10m/s \leq v \leq 30m/s$. The patrol velocity was held constant at $15m/s$. The forward problem is simulated with a uniform cartesian grid of 90 volumes in each direction and the switched grid with 30 volumes in each direction for the reduced dimensional estimator.

A. Stationary source

A stationary source is placed at the center of the $4km \times 4km$ domain. The source releases $1kg/s$ of material into the domain that has a diffusivity of $20m^2/s$ and a $5m/s$ wind going from West to East and South to North. Utilizing the a priori knowledge of the wind, the sensor begins by patrolling the downwind area of the domain.

Figure 5 shows the trajectory of the MSA as it travels through the domain. The sensor detects the source after approximately $97s$ and begins estimating the state of the domain and traveling towards the source. In total, $350s$ were simulated.

Algorithm 3 Sensor-based grid switching

estimate $(X, Y, \psi)_c$
calculate nearest switched grid
if nearest grid = current grid **then**
  do not switch grid
else
  switch grid to nearest grid
  switch spatial operator $\mathcal{A}$
  prolongate state information to general grid
  restrict state information to nearest grid
end if

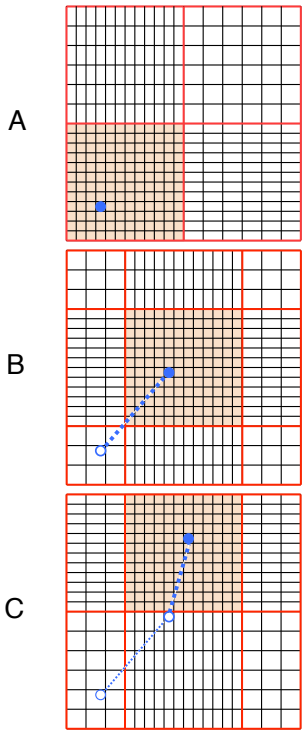

Fig. 4. Sensor-based grid adaptation and switching. Grid refinement is adapted to the sensor current location; sensor commences in shaded area in sub-figure A. Sensor moves to shaded area and grid adjusts around the sensor as in sub-figure B. Sensor moves in a northeastern direction and grid is locally refined around sensor, as in sub-figure C.

B. Moving source: diagonal trajectory

A simple moving source is examined that travels through the domain along the diagonal. The state parameters are the same as in the stationary source case, with the simulation time extended to $500s$. This yields a source speed of approximately $10m/s$. The MSA detects the source approximately $240s$ into the simulation.

C. Moving source: arc trajectory

An arcing source trajectory is simulated where the source enters the domain and releases material as it turns around

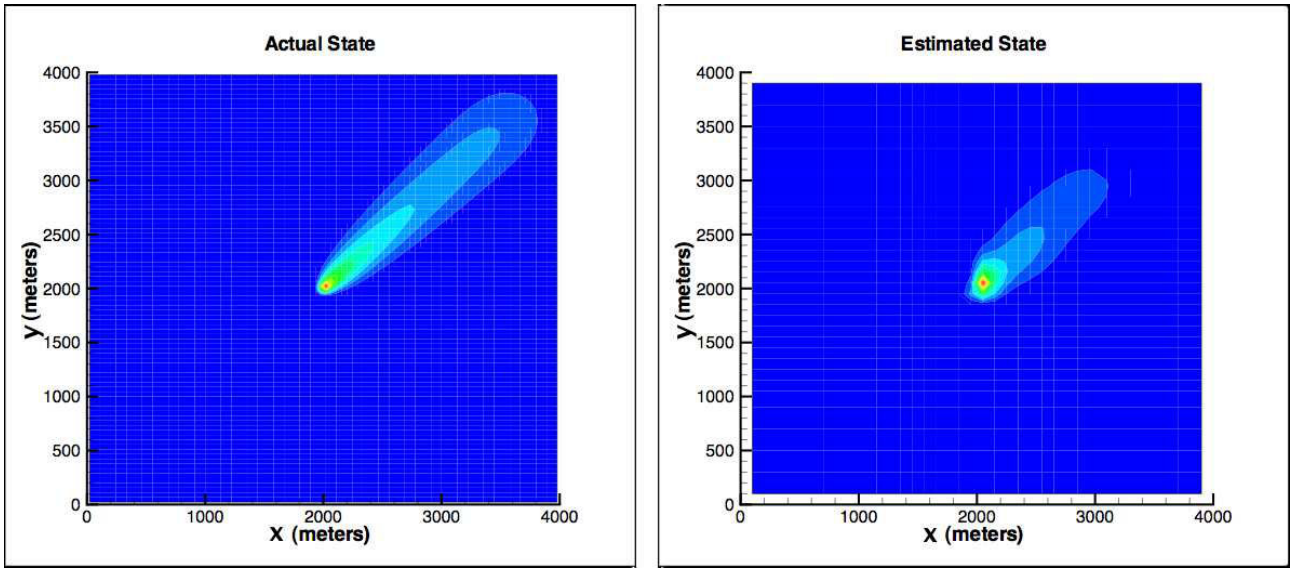

Fig. 6. Comparison of actual and estimated state for a stationary source.

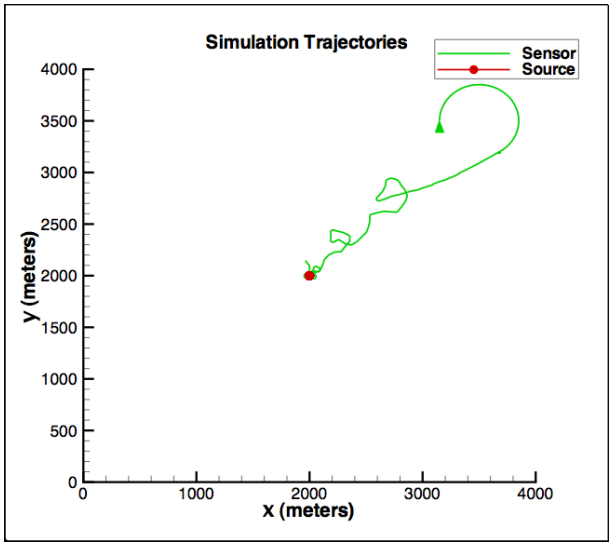

Fig. 5. Source and sensor trajectory for a stationary source.

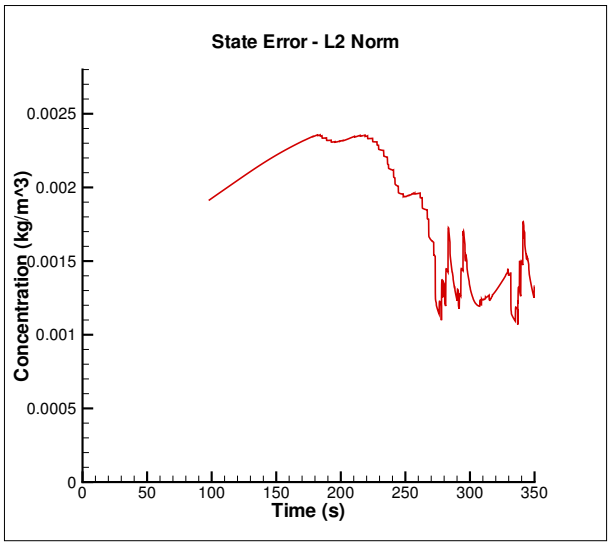

Fig. 7. Evolution of the L^2 norm of the state for a stationary source.

to return from the direction it came from. The atmospheric parameters are the same as for the diagonal case. For this particular source trajectory and patrol path, the MSA detects the source after $40s$.

D. Moving source: overlapping trajectory

A simple overlapping trajectory is examined in which the source's path crosses over itself as shown in Figure 10. The wind was reduced to $1.5m/s$ East to West and $1.0m/s$ South to North so that this particular trajectory creates an area of high concentration at lowermost part of the trajectory.

From the sensor's trajectory, one can observe that the sensor makes a couple of loops in this area of high concentration, then continues to follow the path of the source, where the state error is highest.

VII. Conclusions

A model-based scheme for the detection of the proximity of the location of a moving chemical source in 2D spatial domain was proposed. This detection was realized via the aid of a guided mobile agent equipped with a sensor. Using Lyapunov-based method, a stable guidance scheme is provided for the spatial relocation of the moving sensor. The mobile agent kinematics are also considered and accept as their control input the desired relocation that is dictated by the estimation scheme. Additionally, the proposed estimation scheme with integrated sensor guidance and agent kinematics is coupled to grid refinement. A priori selected combinations of coarse and refined subgrids are switched according to the current sensor location. Computational results served to

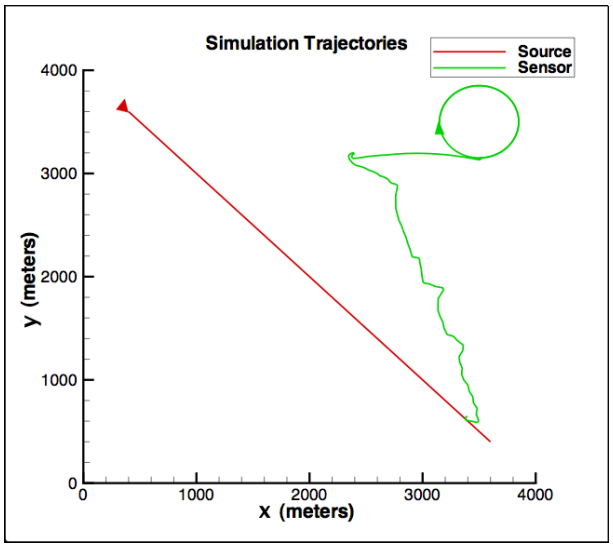

Fig. 8. Source and sensor trajectory for a diagonal source trajectory.

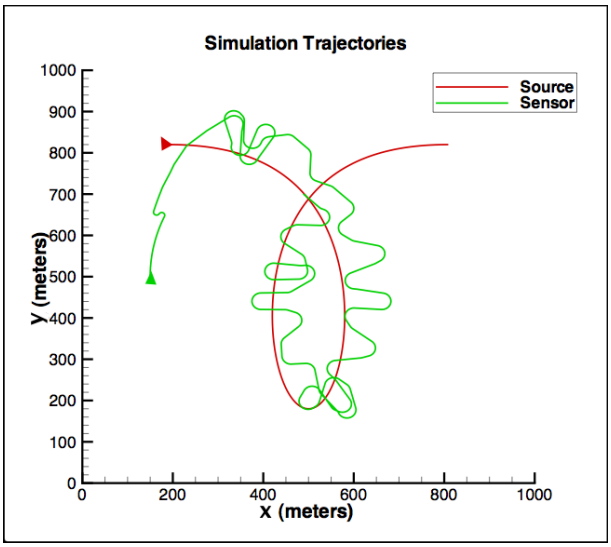

Fig. 10. Source and sensor trajectory for an overlapping source trajectory.

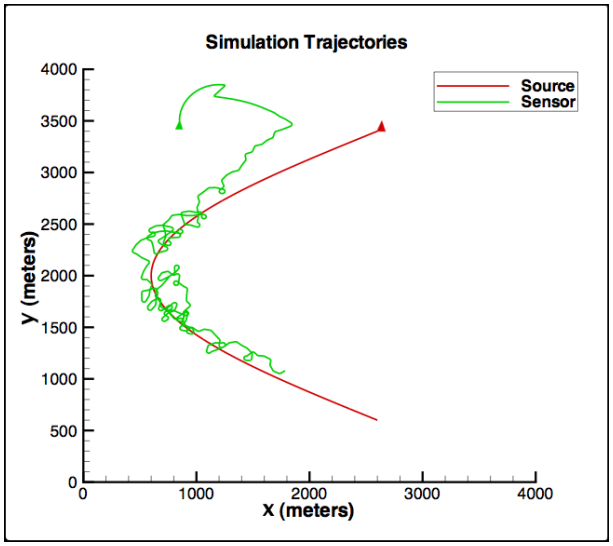

Fig. 9. Source and sensor trajectory for an arcing source trajectory.

demonstrate the effectiveness of the method for 2D spatial domains and realistic parameters for the source, mobile agent, and ambient conditions.

REFERENCES

[1] M. E. Alpay and M. H. Shor, "Model-based solution techniques for the source localization problem," *IEEE Transactions on Control Systems Technology*, vol. 8, no. 6, November 2000.

[2] P. Tzanos and M. Žefran, "Locating a circular biochemical source: Modeling and control," in *Proc. of the 2007 IEEE Int'l Conference on Robotics and Automation*, Roma, Italy, April 10-14 2007.

[3] A. Lilienthal, H. Ulmer, H. Frohlich, A. S. A. amd F. Werner, and A. Zell, "Gas source declaration with a mobile robot," in *Proceedings of the 2004 IEEE International Conference on Robotics & Automation*, New Orleans, LA, April, 2004.

[4] M. A. Demetriou, "Centralized and decentralized policies for the containment of moving source in 2d diffusion processes using sensor/actuator network," in *Proc. of the 2009 American Control Conf.*, St. Louis, MO, June 10-12 2009.

[5] M. A. Demetriou and N. A. Gatsonis, "Scheduling of static sensor networks and management of mobile sensor networks for the detection and containment of moving sources in spatially distributed processes," in *Proc. of the 17th Mediterranean Conference on Control and Automation*, Thessaloniki, Greece, June 24-26 2009.

[6] M. A. Demetriou, "Power management of sensor networks for detection of a moving source in 2-D spatial domains," in *Proc. of the 2006 American Control Conference*, Minneapolis, Minnesota, USA, June 14-16 2006.

[7] ——, "Guidance of mobile actuator-plus-sensor networks for improved control and estimation of distributed parameter systems," *IEEE Tr. on Automatic Control*, vol. 55(7), pp. 1570–1584, 2010.

[8] ——, "Detection and containment policy of moving source in 2-d diffusion processes using sensor/actuator network," in *Proc. of the 2007 European Control Conference (ECC'07)*, Kos, Greece, July 2-5 2007.

[9] J. H. Seinfeld and S. N. Pandis, *Atmospheric Chemistry and Physics: From Air Pollution to Climate Change*. New York: Wiley-Interscience, 2006.

[10] S. P. Arya, *Air Pollution Meteorology and Dispersion*. New York: Oxford University Press, 1999.

[11] R. A. Dobbins, *Atmospheric Motion and Air Pollution*. New York: Wiley, 1979.

[12] W. Ren and R. W. Beard, "Trajectory tracking for unmanned air vehicles with velocity and heading rate constraints," *IEEE Tr. on Contr. Sys. Tech.*, vol. 12(5), pp. 706–716, Sept. 2004.

[13] B. Siciliano and O. Khatib, Eds., *Springer Handbook of Robotics*, Berlin, Heidelberg.

[14] G. Duvaud and J. Lions, *Inequalities in Mechanics & Physics*. New York: Springer-Verlag, 1976.

[15] J. L. Lions and E. Magenes, *Non-Homogeneous Boundary Value Problems, I*. New York: Springer-Verlag, 1972.

[16] R. Temam, *Infinite Dimensonal Dynamical Systems in Mechanics and Physics*, 2nd ed. New York: Springer-Verlag, 1997.

[17] R. A. Adams, *Sobolev Spaces*. NY: Academic Press, 1975.

[18] C. Hirsch, *Numerical Computation of Internal & External Flows*. Oxford, GB: Butterworth-Heinemann, 2007.

[19] N. A. Gatsonis, M. Demagistris, and R. Erlandson, "Three-dimensional magnetohydrodynamic modeling of plasma jets in north star space experiment," *Journal of Spacecraft and Rockets*, vol. 41, no. 4, pp. 509–520, July Aug 2004.